Chapter 5
High-Order CESE Schemes

This chapter is dedicated to the description of high-order CESE schemes. In the second-order CESE schemes, the first-order Taylor expansion was employed to approximate the unknowns and fluxes within the solution elements. The accuracy of the scheme mainly depends on the approximations on the surfaces of the conservation elements. Analogously, the high-order CESE schemes with Mth-order in space and time are generally derived from $(M-1)$th-order Taylor expansions in the solution elements. The high-order CESE schemes use a highly compact stencil. Furthermore, spatial and temporal high-order accuracy can be achieved simultaneously. We shall start with constructing a 1D high-order scheme and then extend it to multi-dimensional schemes.

5.1 Construction of High-Order CESE Schemes

Several attempts have been made to obtain higher-order accuracy for CESE schemes. One of the primary advantages of the high-order CESE schemes is the usage of the most compact stencil. High-order accuracy is achieved by the approximation with high-order Taylor expansions. For example, $a(3)$ scheme [1] has 4th order of accuracy by applying second-order Taylor expansion, and it is stable for $v < 0.5$. Furthermore, $a(4)$ scheme [2] with 4th to 5th order of accuracy was developed by defining more CEs at each grid point. The CFL number needs to be constrained below 1/3. The constructions of high-order schemes from the above two approaches were limited to only 1D scenarios. Alternatively, Chang [3] proposed a high-order scheme that can be extended to arbitrary order with CFL limited below 1. In this scheme, the even derivatives are advanced in the same manner as the conserved variables, whereas the odd derivatives are advanced through finite difference. This method has been extended to solve Euler equations [4]. In this section, we follow the approaches of Liu and Wang [5] in deriving the high-order 1D scheme, Wang et al. [6] for 2D high-order

C.-Y. Wen et al., *Space–Time Conservation Element and Solution Element Method*,
Engineering Applications of Computational Methods 13,
https://doi.org/10.1007/978-981-99-0876-9_5

schemes on uniform meshes, and Shen et al. [7] for the 2D high-order scheme for hybrid meshes. In these schemes, only the conserved variables are computed through the integration on the CE surfaces, while all the physical derivatives are computed through the finite difference of lower-order derivatives. In the following text, we will present the constructions of the third-order CESE schemes. The construction of arbitrary order schemes could be achieved by implementing the same strategy, and details can be accessed in Shen et al. [7] and Yang et al. [8].

5.1.1 Construction of a Third-Order 1D CESE Scheme

Recall the 1D scalar problem

$$\frac{\partial u}{\partial t} + \frac{\partial f(u)}{\partial x} = 0 \tag{5.1}$$

with $f = au$. To formulate a third-order scheme, $u(x, t)$ and $f(x, t)$ in any $(x, t) \in \mathrm{SE}(j, n)$ are approximated by the second-order Taylor expansion as

$$\begin{aligned} u(x,t) = {} & u_j^n + (u_x)_j^n (x - x_j) + (u_t)_j^n (t - t_n) + (u_{xt})_j^n (x - x_j)(t - t_n) \\ & + \frac{1}{2}(u_{xx})_j^n (x - x_j)^2 + \frac{1}{2}(u_{tt})_j^n (t - t_n)^2, \quad (x,t) \in (\mathrm{SE})_j^n \end{aligned} \tag{5.2}$$

$$\begin{aligned} f(x,t) = {} & f_j^n + (f_x)_j^n (x - x_j) + (f_t)_j^n (t - t_n) + (f_{xt})_j^n (x - x_j)(t - t_n) \\ & + \frac{1}{2}(f_{xx})_j^n (x - x_j)^2 + \frac{1}{2}(f_{tt})_j^n (t - t_n)^2. \quad (x,t) \in (\mathrm{SE})_j^n \end{aligned} \tag{5.3}$$

where u_{xt}, u_{xx}, u_{tt}, f_{xt}, f_{xx}, and f_{tt} are the second-order derivatives of u and f, respectively. These derivatives are assumed constant within the SE. With the aid of the Eqs. (5.1) and (5.2), then one has

$$(u_t)_j^n = -a(u_x)_j^n, \quad (u_{xt})_j^n = -a(u_{xx})_j^n, \quad (u_{tt})_j^n = a^2(u_{xx})_j^n. \tag{5.4}$$

It implies that u, u_x, u_{xx} are the only independent variables associated with each grid point. Substituting Eqs. (5.2) and (5.3) into the integral form of Eq. (5.1). The following algebraic relation can be derived as

$$u_j^n \Delta x + (u_{xx})_j^n \frac{\Delta x^3}{24} = U_L + U_R + F_L - F_R, \tag{5.5}$$

where

$$\begin{aligned} U_L &= \tfrac{\Delta x}{2} u_{j-1/2}^{n-1/2} + \tfrac{\Delta x^2}{8} (u_x)_{j-1/2}^{n-1/2} + \tfrac{\Delta x^3}{48} (u_{xx})_{j-1/2}^{n-1/2} \\ U_R &= \tfrac{\Delta x}{2} u_{j+1/2}^{n-1/2} - \tfrac{\Delta x^2}{8} (u_x)_{j+1/2}^{n-1/2} + \tfrac{\Delta x^3}{48} (u_{xx})_{j+1/2}^{n-1/2} \\ F_L &= \tfrac{\Delta t}{2} f_{j-1/2}^{n-1/2} + \tfrac{\Delta t^2}{8} (f_t)_{j-1/2}^{n-1/2} + \tfrac{\Delta t^3}{48} (f_{tt})_{j-1/2}^{n-1/2} \\ F_R &= \tfrac{\Delta t}{2} f_{j+1/2}^{n-1/2} + \tfrac{\Delta t^2}{8} (f_t)_{j+1/2}^{n-1/2} + \tfrac{\Delta t^3}{48} (f_{tt})_{j+1/2}^{n-1/2} \end{aligned} . \tag{5.6}$$

In Eqs. (5.5) and (5.6), the values at $t = t_{n-1/2}$ are already known. It is necessary to calculate $(u_{xx})_j^n$ at $t = t_n$ before explicitly computing u_j^n. The second-order derivative, $(u_{xx})_j^n$, is approximated by a central difference as

$$(u_{xx})_j^n = \frac{(u_x)_{j+1/2}^n - (u_x)_{j-1/2}^n}{\Delta x}. \tag{5.7}$$

Then u_j^n can be directly computed from Eq. (5.5), and $(u_x)_j^n$ can be calculated in the same manner as the second-order a-α schemes using the weighted average function.

5.1.2 Construction of a Third-Order 2D CESE Scheme on Uniform Mesh

Recall the 2D scalar hyperbolic conservation law

$$\frac{\partial u}{\partial t} + \frac{\partial f}{\partial x} + \frac{\partial g}{\partial y} = 0. \tag{5.8}$$

which can be cast into the integral form

$$\oint_{S(\mathrm{CE}(P'))} \boldsymbol{h} \cdot \boldsymbol{n} \, \mathrm{d}S = 0 \tag{5.9}$$

where $\boldsymbol{h} = (f, g, u)$ is the space–time flux vector, $\boldsymbol{n}$ is the unit outward normal vector on the surface of the control volume. Inspired by the construction of the high-order 1D scheme, second-order Taylor expansion is utilized inside the SE to estimate u, f, and g. The definitions of SE and CE are kept the same as the second-order schemes (Fig. 4.1). For a point (x, y, t) that belongs to SE(P'),

$$u(x, y, t) = u(\delta x, \delta y, \delta t)_{P'}, \quad (x, y, t) \in \mathrm{SE}\left(P'\right) \tag{5.10}$$

$$f(x, y, t) = f(\delta x, \delta y, \delta t)_{P'}, \quad (x, y, t) \in \mathrm{SE}\left(P'\right) \tag{5.11}$$

$$g(x, y, t) = g(\delta x, \delta y, \delta t)_{P'}, \quad (x, y, t) \in \mathrm{SE}\left(P'\right) \tag{5.12}$$

where $X(\delta x, \delta y, \delta t)_N$ denotes the second-order Taylor expansion about point N as

$$\begin{aligned} X(\delta x, \delta y, \delta t)_N = X_N + (X_x)_N \delta x + \left(X_y\right)_N \delta y + (X_t)_N \delta t \\ + \frac{1}{2}(X_{xx})_N (\delta x)^2 + \frac{1}{2}\left(X_{yy}\right)_N (\delta y)^2 + \frac{1}{2}(X_{tt})_N (\delta t)^2 \\ + \left(X_{xy}\right)_N \delta x \delta y + \left(X_{yt}\right)_N \delta y \delta t + (X_{xt})_N \delta x \delta t. \end{aligned} \tag{5.13}$$

and

$$\delta x = x - x_N, \ \delta y = y - y_N, \ \delta t = t - t_N. \tag{5.14}$$

Substituting Eqs. (5.10)–(5.12) into (5.8), one obtains

$$\begin{aligned} u_t &= -f_x - g_y \\ u_{tt} &= -f_{xt} - g_{yt} \\ u_{xt} &= -f_{xx} - g_{xy} \\ u_{yt} &= -f_{xy} - g_{yy} \end{aligned}. \tag{5.15}$$

Together with the chain rule, to compute the derivatives in Eq. (5.13), the only unknowns are u, u_x, u_y, u_{xx}, u_{yy}, and u_{xy}. By integrating over the surface of the CE(P'), Eq. (5.9) leads to

$$\begin{aligned} \oint_{S(V)} \boldsymbol{h} \cdot \boldsymbol{n} \, \mathrm{d}S = \int_{A'B'C'D'} \boldsymbol{h} \cdot \boldsymbol{n} \, \mathrm{d}S + \int_{ABCD} \boldsymbol{h} \cdot \boldsymbol{n} \, \mathrm{d}S + \int_{ABB'A'} \boldsymbol{h} \cdot \boldsymbol{n} \, \mathrm{d}S \\ + \int_{BCC'B'} \boldsymbol{h} \cdot \boldsymbol{n} \, \mathrm{d}S + \int_{CDD'C'} \boldsymbol{h} \cdot \boldsymbol{n} \, \mathrm{d}S + \int_{DAA'D'} \boldsymbol{h} \cdot \boldsymbol{n} \, \mathrm{d}S = 0. \end{aligned} \tag{5.16}$$

Thereafter, with the aid of Eqs. (5.10) –(5.12) and (5.16) can be rearranged as

$$(u)_{p'} + \frac{(\Delta x)^2}{24}(u_{xx})_{p'} + \frac{(\Delta y)^2}{24}\left(u_{yy}\right)_{p'} = \frac{1}{4}\left(\overline{u} + \frac{\Delta t}{\Delta x}\overline{f} + \frac{\Delta t}{\Delta y}\overline{g}\right), \tag{5.17}$$

where

$$\begin{aligned} \bar{u} =& \hat{u}\left(\frac{\Delta x}{4}, \frac{\Delta y}{4}, 0\right)_A + \hat{u}\left(-\frac{\Delta x}{4}, \frac{\Delta y}{4}, 0\right)_B \\ &+ \hat{u}\left(-\frac{\Delta x}{4}, -\frac{\Delta y}{4}, 0\right)_C + \hat{u}\left(\frac{\Delta x}{4}, -\frac{\Delta y}{4}, 0\right)_D, \\ \bar{f} =& \hat{f}\left(0, \frac{\Delta y}{4}, \frac{\Delta t}{4}\right)_A - \hat{f}\left(0, \frac{\Delta y}{4}, \frac{\Delta t}{4}\right)_B \end{aligned} \tag{5.18}$$

$$- \hat{f}\left(0, -\frac{\Delta y}{4}, \frac{\Delta t}{4}\right)_C + \hat{f}\left(0, -\frac{\Delta y}{4}, \frac{\Delta t}{4}\right)_D, \tag{5.19}$$

$$\begin{aligned}\bar{g} =& \hat{g}\left(\frac{\Delta x}{4}, 0, \frac{\Delta t}{4}\right)_A + \hat{g}\left(-\frac{\Delta x}{4}, 0, \frac{\Delta t}{4}\right)_B \\ & - \hat{g}\left(-\frac{\Delta x}{4}, 0, \frac{\Delta t}{4}\right)_C - \hat{g}\left(\frac{\Delta x}{4}, 0, \frac{\Delta t}{4}\right)_D,\end{aligned} \tag{5.20}$$

and

$$\begin{aligned}\hat{u}(\delta x, \delta y, \delta t)_N =& (u)_N + (u_x)_N \delta x + \left(u_y\right)_N \delta y + (u_t)_N \delta t \\ & + \frac{1}{6}(u_{xx})_N (\delta x)^2 + \frac{1}{6}\left(u_{yy}\right)_N (\delta y)^2 + \left(u_{xy}\right)_N \delta x \delta y,\end{aligned} \tag{5.21}$$

$$\begin{aligned}\hat{f}(\delta x, \delta y, \delta t)_N =& (f)_N + (f_x)_N \delta x + \left(f_y\right)_N \delta y + (f_t)_N \delta t \\ & + \frac{1}{6}\left(f_{yy}\right)_N (\delta y)^2 + \frac{1}{6}(f_{tt})_N (\delta t)^2 + \left(f_{yt}\right)_N \delta y \delta t,\end{aligned} \tag{5.22}$$

$$\begin{aligned}\hat{g}(\delta x, \delta y, \delta t)_N =& (g)_N + (g_x)_N \delta x + \left(g_y\right)_N \delta y + (g_t)_N \delta t \\ & + \frac{1}{6}(g_{xx})_N (\delta x)^2 + \frac{1}{6}(g_{tt})_N (\delta t)^2 + (g_{xt})_N \delta x \delta t.\end{aligned} \tag{5.23}$$

Prior to explicitly computing $(u)_{p'}$ from Eq. (5.17), $(u_{xx})_{p'}$ and $\left(u_{yy}\right)_{p'}$ are required to be obtained from the finite difference of the interpolations from the previous time step. The second-order derivative $(u_{xx})_{p'}$ can be estimated as

$$(u_{xx})^+_{p'} = \frac{(u_x)_B + \frac{\Delta t}{2}(u_{xt})_B - (u_x)_A - \frac{\Delta t}{2}(u_{xt})_A}{\Delta x}, \tag{5.24}$$

$$(u_{xx})^-_{p'} = \frac{(u_x)_C + \frac{\Delta t}{2}(u_{xt})_C - (u_x)_D - \frac{\Delta t}{2}(u_{xt})_D}{\Delta x}. \tag{5.25}$$

$(u_{xx})_{p'}$ is then computed from simple average as

$$(u_{xx})_{p'} = \frac{(u_{xx})^+_{p'} + (u_{xx})^-_{p'}}{2}. \tag{5.26}$$

Similarly, the derivative $\left(u_{yy}\right)_{p'}$ is computed as

$$\left(u_{yy}\right)^+_{p'} = \frac{\left(u_y\right)_D + \frac{\Delta t}{2}\left(u_{yt}\right)_D - \left(u_y\right)_A - \frac{\Delta t}{2}\left(u_{yt}\right)_A}{\Delta y}, \tag{5.27}$$

$$\left(u_{yy}\right)_{p'}^{-} = \frac{\left(u_y\right)_C + \frac{\Delta t}{2}\left(u_{yt}\right)_C - \left(u_y\right)_B - \frac{\Delta t}{2}\left(u_{yt}\right)_B}{\Delta y}, \tag{5.28}$$

$$\left(u_{yy}\right)_{p'} = \frac{\left(u_{yy}\right)_{p'}^{+} + \left(u_{yy}\right)_{p'}^{-}}{2}. \tag{5.29}$$

Equations (5.17), (5.26), and (5.29) form the procedure to get the values of $(u)_{p'}$, $(u_{xx})_{p'}$ and $\left(u_{yy}\right)_{p'}$ at the new time level. To complete the time marching, we need to further compute u_x, u_y, and u_{xy}. The weighted average of the sided-estimations computes the first-order derivatives as

$$(u_x)_{p'}^{+} = \frac{1}{\Delta x}\left[u\left(0, 0, \frac{\Delta t}{2}\right)_B + u\left(0, 0, \frac{\Delta t}{2}\right)_C - 2(u_x)_{p'}\right], \tag{5.30}$$

$$(u_x)_{p'}^{-} = \frac{1}{\Delta x}\left[2(u_x)_{p'} - u\left(0, 0, \frac{\Delta t}{2}\right)_A - u\left(0, 0, \frac{\Delta t}{2}\right)_D\right], \tag{5.31}$$

$$\left(u_y\right)_{p'}^{+} = \frac{1}{\Delta y}\left[u\left(0, 0, \frac{\Delta t}{2}\right)_C + u\left(0, 0, \frac{\Delta t}{2}\right)_D - 2(u_x)_{p'}\right], \tag{5.32}$$

$$\left(u_y\right)_{p'}^{-} = \frac{1}{\Delta y}\left[2\left(u_y\right)_{p'} - u\left(0, 0, \frac{\Delta t}{2}\right)_A - u\left(0, 0, \frac{\Delta t}{2}\right)_B\right], \tag{5.33}$$

$$(u_x)_{p'} = W\left(\left(u_x^{-}\right)_{P'}, \left(u_x^{+}\right)_{P'}, \alpha\right), \tag{5.34}$$

$$\left(u_y\right)_{p'} = W\left(\left(u_y^{-}\right)_{P'}, \left(u_y^{+}\right)_{P'}, \alpha\right). \tag{5.35}$$

Meanwhile, the mixed derivative u_{xy} is computed from

$$\left(u_{xy}\right)_{p'}^{+} = \frac{(u_x)_D + \frac{\Delta t}{2}(u_{xt})_D - (u_x)_A - \frac{\Delta t}{2}(u_{xt})_A}{\Delta y}, \tag{5.36}$$

$$\left(u_{xy}\right)_{p'}^{-} = \frac{(u_x)_C + \frac{\Delta t}{2}(u_{xt})_C - (u_x)_B - \frac{\Delta t}{2}(u_{xt})_B}{\Delta y}, \tag{5.37}$$

$$\left(u_{yx}\right)_{p'}^{+} = \frac{(u_x)_B + \frac{\Delta t}{2}(u_{xt})_B - (u_x)_A - \frac{\Delta t}{2}(u_{xt})_A}{\Delta x}, \tag{5.38}$$

$$\left(u_{yx}\right)_{p'}^{-} = \frac{(u_x)_C + \frac{\Delta t}{2}(u_{xt})_C - (u_x)_D - \frac{\Delta t}{2}(u_{xt})_D}{\Delta x}, \tag{5.39}$$

$$\left(u_{xy}\right)_{p'} = \frac{1}{4}\left[\left(u_{xy}\right)_{p'}^{+} + \left(u_{xy}\right)_{p'}^{-} + \left(u_{yx}\right)_{p'}^{+} + \left(u_{yx}\right)_{p'}^{-}\right]. \tag{5.40}$$

5.1.3 Construction of a Third-Order 2D CESE Scheme on Unstructured Mesh

Similar to constructing the third-order scheme on a a uniform mesh, second-order Taylor expansion is utilized here, and the variables stored at each grid point are still $u, u_x, u_y, u_{xx}, u_{yy}$, and u_{xy}. Now we recollect the definitions of SE and CE in the 2D CESE scheme on the unstructured mesh as depicted in Fig. 4.4, and the flux balancing relation was derived in Eq. (4.48). From the summation of the conservation law for all the sub-CEs, we arrive at the flux balancing relation for CE($V_i^{'}$):

$$\iint\limits_{C_1^{'}O_1^{'}\cdots C_M^{'}O_M^{'}} u\, d\sigma = \sum_{m=1}^{M} \iint\limits_{C_m O_m V_i O_{m-1}} u\, d\sigma - \sum_{m=1}^{M} \iint\limits_{C_m O_m O_m^{'} C_m^{'} + O_{m-1} C_m C_m^{'} O_{m-1}^{'}} \mathbf{V}\cdot\mathbf{n} d\sigma. \tag{5.41}$$

The LHS of Eq. (5.41) represents the integration of u on the top surface of CE($V_i^{'}$), i.e.,

$$\begin{aligned}\iint\limits_{C_1^{'}O_1^{'}\cdots C_M^{'}O_M^{'}} u\, d\sigma &= u(G_i^{'})\cdot S + \text{TERM1} = u(G_i^{'})\cdot S + \sum_{m=1}^{M} \iint\limits_{C_m^{'} O_m^{'} G_i^{'} O_{m-1}^{'}} \frac{1}{2}\frac{\partial^2 u(G_i^{'})}{\partial x^2}(\delta x)^2 \\ &+ \frac{1}{2}\frac{\partial^2 u(G_i^{'})}{\partial y^2}(\delta y)^2 + \frac{\partial^2 u(G_i^{'})}{\partial x \partial y}(\delta x)(\delta y) dx dy,\end{aligned} \tag{5.42}$$

where $\delta x = x - x(G_i^{'})$, $\delta y = y - y(G_i^{'})$, and S represents the area of the polygon $C_1^{'}O_1^{'}\ldots C_M^{'}O_M^{'}$. The second term in RHS (TERM1) of Eq. (5.42) denotes the integration of the high-order terms of u. The two terms in RHS of Eq. (5.41) can be respectively expressed as

$$\begin{aligned}\sum_{m=1}^{M} \iint\limits_{C_m O_m V_i O_{m-1}} u\, d\sigma &= \text{TERM2} = \sum_{m=1}^{M} \iint\limits_{C_m O_m V_i O_{m-1}} u(C_m) + \frac{\partial u(C_m)}{\partial x}(\delta x) + \frac{\partial u(C_m)}{\partial y}(\delta y) \\ &+ \frac{1}{2}\frac{\partial^2 u(C_m)}{\partial x^2}(\delta x)^2 + \frac{1}{2}\frac{\partial^2 u(C_m)}{\partial y^2}(\delta y)^2 + \frac{\partial^2 u(C_m)}{\partial x \partial y}(\delta x)(\delta y) dx dy,\end{aligned} \tag{5.43}$$

where $\delta x = x - x(C_m)$, $\delta y = y - y(C_m)$.

$$\sum_{m=1}^{M} \iint\limits_{C_m O_m O_m^{'} C_m^{'} + O_{m-1} C_m C_m^{'} O_{m-1}^{'}} \mathbf{V}\cdot\mathbf{n} d\sigma = \text{TERM3} = \sum_{m=1}^{M} \left[FLUX_1^{(m)} + FLUX_2^{(m)} \right], \tag{5.44}$$

with

$$FLUX_1^{(m)} = \frac{\Delta t}{2}\Delta y_1^{(m)} \sum_{a=0}^{2}\sum_{b=0}^{2-a}\sum_{c=0}^{2-a-b} \frac{1}{(a+b+1)a!b!(c+1)!} \frac{\partial^{a+b+c} f(C_m)}{\partial x^a \partial y^b \partial t^c} \left[\Delta x_1^{(m)}\right]^a \left[\Delta y_1^{(m)}\right]^b \left[\frac{\Delta t}{2}\right]^c - \frac{\Delta t}{2}\Delta x_1^{(m)} \sum_{a=0}^{2}\sum_{b=0}^{2-a}\sum_{c=0}^{2-a-b} \frac{1}{(a+b+1)a!b!(c+1)!} \frac{\partial^{a+b+c} g(C_m)}{\partial x^a \partial y^b \partial t^c} \left[\Delta x_1^{(m)}\right]^a \left[\Delta y_1^{(m)}\right]^b \left[\frac{\Delta t}{2}\right]^c, \tag{5.45}$$

$$FLUX_2^{(m)} = \frac{\Delta t}{2}\Delta y_2^{(m)} \sum_{a=0}^{2}\sum_{b=0}^{2-a}\sum_{c=0}^{2-a-b} \frac{1}{(a+b+1)a!b!(c+1)!} \frac{\partial^{a+b+c} f(C_m)}{\partial x^a \partial y^b \partial t^c} \left[-\Delta x_2^{(m)}\right]^a \left[-\Delta y_2^{(m)}\right]^b \left[\frac{\Delta t}{2}\right]^c - \frac{\Delta t}{2}\Delta x_2^{(m)} \sum_{a=0}^{2}\sum_{b=0}^{2-a}\sum_{c=0}^{2-a-b} \frac{1}{(a+b+1)a!b!(c+1)!} \frac{\partial^{a+b+c} g(C_m)}{\partial x^a \partial y^b \partial t^c} \left[-\Delta x_2^{(m)}\right]^a \left[-\Delta y_2^{(m)}\right]^b \left[\frac{\Delta t}{2}\right]^c, \tag{5.46}$$

in which $\Delta x_1^{(m)} = x(O_m) - x(C_m)$, $\Delta y_1^{(m)} = y(O_m) - y(C_m)$, $\Delta x_2^{(m)} = x(C_m) - x(O_{m-1})$, $\Delta y_2^{(m)} = y(C_m) - y(O_{m-1})$. $FLUX^{(m)}{}_1$ and $FLUX^{(m)}{}_2$ represent the fluxes across the adjacent CE surfaces on which the points are defined within SE(C_m).

By substituting Eqs. (5.42)–(5.44) into (5.41) and moving the high-order terms to RHS. Consequently, the value of $u(G_i^{'})$ can be expressed by

$$u\left(G_i'\right) = \frac{1}{S}(\text{TERM2} - \text{TERM3} - \text{TERM1}). \tag{5.47}$$

Two remarks should be noted regarding Eq. (5.47). First of all, since u, f, and g are nonlinearly distributed on the surfaces of CE, the integral terms appeared in Eqs. (5.42) and (5.43) are not simple multiplications of the value at the centroid and the surface area as what has been implemented in the second-order scheme. In contrast, they are now calculated using the coordinate transformation method:

$$x = \sum_{i=1}^{4} x_i N_i(\xi,\ \eta), \tag{5.48}$$

$$y = \sum_{i=1}^{4} y_i N_i(\xi,\ \eta), \tag{5.49}$$

where

$$N_1 = \frac{1}{4}(1-\xi)(1-\eta), \qquad N_2 = \frac{1}{4}(1+\xi)(1-\eta),$$
$$N_3 = \frac{1}{4}(1+\xi)(1+\eta), \qquad N_4 = \frac{1}{4}(1-\xi)(1+\eta). \tag{5.50}$$

Thereafter, the integration of an arbitrary function $\phi(x, y)$ over the irregular quadrangle A is transformed into the integration over a rectangle (Fig. 5.1) as

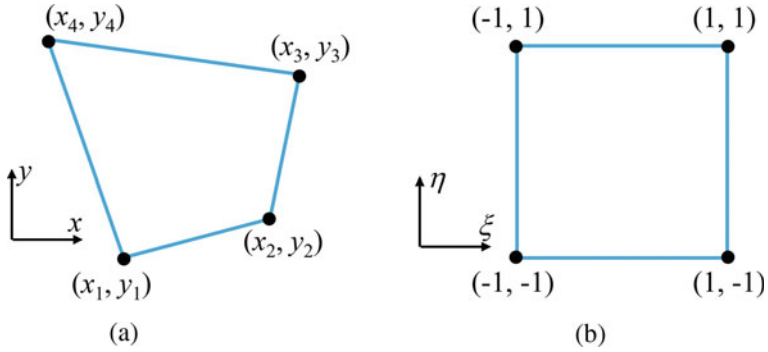

Fig. 5.1 Sketch of the coordinate transformation

$$\iint_A \phi(x, y)ds = \int_{-1}^{1} d\eta \int_{-1}^{1} \phi[x(\xi, \eta), y(\xi, \eta)]\mathbf{J}d\xi, \tag{5.51}$$

where $\mathbf{J}$ is the Jacobian matrix of the coordinate transformation,

$$\mathbf{J} = \frac{\partial(x, y)}{\partial(\xi, \eta)} = \begin{vmatrix} \sum_{i=1}^{4} x_i \frac{\partial N_i}{\partial \xi} & \sum_{i=1}^{4} y_i \frac{\partial N_i}{\partial \xi} \\ \sum_{i=1}^{4} x_i \frac{\partial N_i}{\partial \eta} & \sum_{i=1}^{4} y_i \frac{\partial N_i}{\partial \eta} \end{vmatrix}. \tag{5.52}$$

In addition, TERM2 and TERM3 in Eq. (5.47) can be computed from the information at $t = t_{n-1/2}$. TERM1 consists of high-order terms (u_{xx}, u_{yy}, and u_{xy}) of u at $t = t_n$. As a result, the high-order derivatives must be solved prior to computing u. The idea to calculate the high-order derivatives are analogue to that in Sects. 5.1.1 and 5.1.2. For example, from the Taylor expansion $C_m^{'}$ we have

$$u_x\left(C'_{m-1}\right) - u_x\left(C'_m\right) = u_{xx}\left(C'_m\right)\left[x(C'_{m-1}) - x(C'_m)\right] + u_{xy}\left(C'_m\right)\left[y(C'_{m-1}) - y(C'_m)\right], \tag{5.53}$$

$$u_x\left(C'_{m+1}\right) - u_x\left(C'_m\right) = u_{xx}\left(C'_m\right)\left[x(C'_{m+1}) - x(C'_m)\right] + u_{xy}\left(C'_m\right)\left[y(C'_{m+1}) - y(C'_m)\right]. \tag{5.54}$$

On the other hand, $u_x(C_{m-1}^{'})$, $u_x(C_m^{'})$, $u_x(C_{m+1}^{'})$ can be interpolated from the previous time level,

$$\begin{aligned} u_x\left(C'_{m-1}\right) &= u_x(C_{m-1}) + u_{xx}(C_{m-1})\frac{\Delta t}{2} \\ u_x\left(C'_m\right) &= u_x(C_m) + u_{xx}(C_m)\frac{\Delta t}{2} \\ u_x\left(C'_{m+1}\right) &= u_x(C_{m+1}) + u_{xx}(C_{m+1})\frac{\Delta t}{2} \end{aligned} \tag{5.55}$$

By substituting Eq. (5.55) into Eqs. (5.53) and (5.54), a pair of equations with two unknowns ($u_{xx}(C_m^{'})$, $u_{xy}(C_m^{'})$) are ready to be solved by Cramer's rule. A simple

average (or weighted average to suppress oscillations near discontinuities) can be applied for M pairs of derivatives. Once all the second-order derivatives are obtained under the same routine, $u(G_i^{'})$ can be immediately calculated from Eq. (5.47). The last unknowns remain to be computed are u_x and u_y, which can be calculated similarly in Sect. 4.2, e.g.,

$$\begin{aligned} &u\left(G_i'\right) + u_x\left(G_i'\right)\delta x + u_y\left(G_i'\right)\delta y + \tfrac{1}{2}u_{xx}\left(G_i'\right)(\delta x)^2 + \tfrac{1}{2}u_{yy}\left(G_i'\right)(\delta y)^2 \\ &+u_{xy}\left(G_i'\right)(\delta x)(\delta y) = u(C_m) + u_t(C_m)\tfrac{\Delta t}{2} + \tfrac{1}{2}u_{tt}(C_m)\left(\tfrac{\Delta t}{2}\right)^2 \end{aligned}, \tag{5.56}$$

where $\delta x = x(C_m) - x(G_i^{'})$, $\delta y = y(C_m) - y(G_i^{'})$. Similarly, on applying Eq. (5.56) to C_{m+1}, a pair of u_x and u_y can be easily determined. Then, we apply the weighted average function to obtain the optimal derivatives. Finally, $u(V_i^{'})$ and its derivatives are interpolated by Taylor expansion from the information at $u(G_i^{'})$.

5.2 Numerical Examples

The Shu-Osher problem consists of a Mach 3 shock interacting with an entropy wave, which requires the capability of capturing fine structures in the flow. The computational domain [0, 10] is discretized by a uniform grid size of 0.05, the non-reflection boundary condition is imposed on both sides, and the initial condition is described as

$$(\rho,\ u,\ p) = \begin{cases} (3.857143,\ 2.629369,\ 10.33333) & x \le 1 \\ (1 + 0.2\sin(5x),\ 0,\ 1) & x > 1 \end{cases} \tag{5.57}$$

The density distributions at $t = 1.8$ are depicted in (Fig. 5.2). Compared to the benchmark solution, which is calculated with a-α scheme using very high grid resolution, higher-order CESE schemes are less dissipative and can reveal better flow structures.

The second example is the Mach 3 wind tunnel problem with step. This problem has been described in Sect. 4.3. Here, we use the identical numerical setups except with a mesh size of 1/250. As depicted in Fig. 5.3, vortex-like structures generated in the results using high-order schemes, however, disappeared in the low-order schemes due to the increasing dissipation. It is not surprising that the triangular mesh result surpasses the quadrilateral ones because the mesh area is only half of the latter when the mesh sizes are the same.

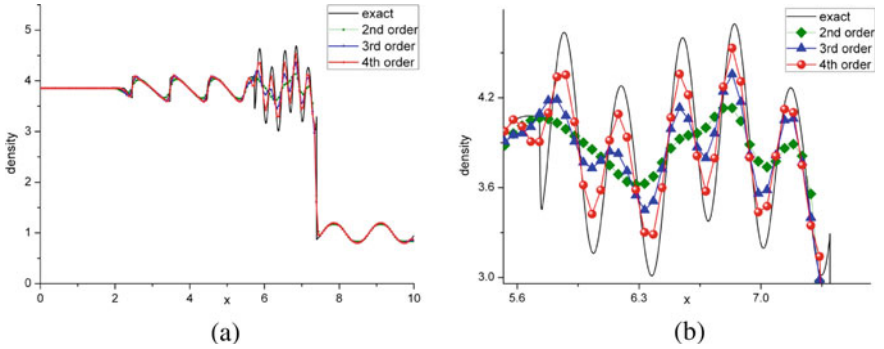

Fig. 5.2 Density distributions for Shu-Osher problem at $t = 1.8$. **a** Entire view, **b** Enlargement. Courtesy of Shen [7]

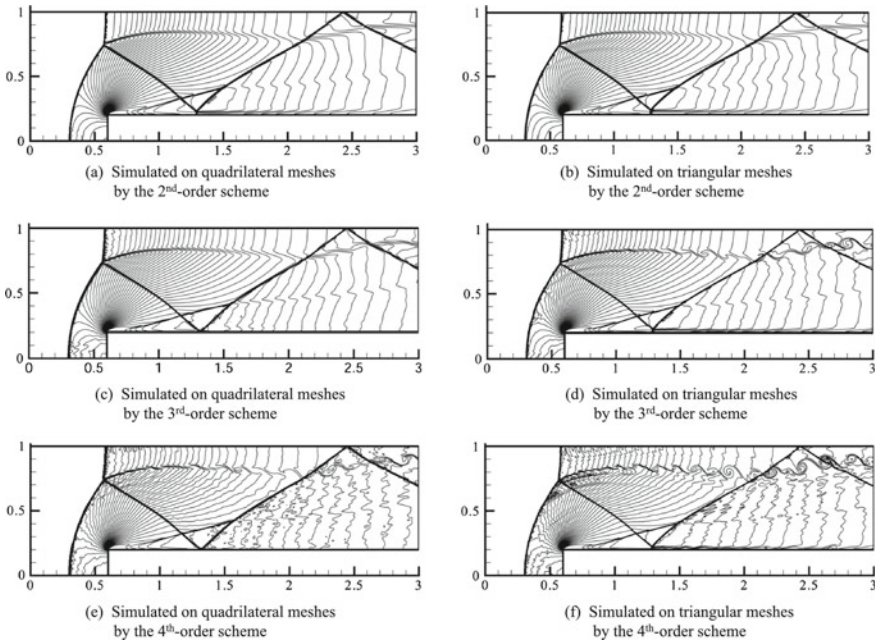

Fig. 5.3 Density contours for Mach 3 wind tunnel with a step at $t = 4.0$. Courtesy of Shen [7]

References

1. Chang, S.C. (2007). The $a(3)$ Scheme: A fourth-order neutrally stable CESE solver. In *18th AIAA Computational Fluid Dynamics Conference.*
2. Chang, S.C. (2009). The $a(4)$ Scheme: A high order neutrally stable CESE solver. In *43rd AIAA/ASME/SAE/ASEE Joint Propulsion Conference & Exhibit*.
3. Chang, S.C. (2010). A new approach for constructing highly stable high order CESE schemes.

In *48th AIAA Aerospace Sciences Meeting Including the New Horizons Forum and Aerospace Exposition.*
4. Bilyeu, D., Chen, Y.Y. & Yu, S.T.J. (2011). High-order CESE methods for the Euler equations. In *49th AIAA Aerospace Sciences Meeting including the New Horizons Forum and Aerospace Exposition.*
5. Liu, K. X., & Wang, J. T. (2004). Analysis of high accuracy conservation-element and solution-element schemes. *Chinese Physics Letters, 21*(11), 2085.
6. Wang, G., Zhang, D. L., & Liu, K. X. (2007). An improved CE/SE scheme and its application to detonation propagation. *Chinese Physics Letters, 24*(12), 3563.
7. Shen, H., Wen, C. Y., Liu, K. X., & Zhang, D. L. (2015). Robust high-order space–time conservative schemes for solving conservation laws on hybrid meshes. *Journal of Computational Physics, 281*, 375–402.
8. Yang, Y., Feng, X. S., & Jiang, C. W. (2017). A high-order CESE scheme with a new divergence-free method for MHD numerical simulation. *Journal of Computational Physics, 349*, 561–581.